Food and Chemical Toxicology 133 (2019) 110731

Contents lists available at ScienceDirect

Food and Chemical Toxicology

journal homepage: www.elsevier.com/locate/foodchemtox

Effect of chitosan on the digestibility and molecular structural properties of lotus seed starch

Mingjing Zheng[a,b], Suzhen Lei[a], Hongqiang Wu[a], Baodong Zheng[a,b], Yi Zhang[a,b,*], Hongliang Zeng[a,b,**]

[a] College of Food Science, Fujian Agriculture and Forestry University, Fuzhou, Fujian, 350002, China
[b] Fujian Province Key Laboratory of Quality Science and Processing Technology in Special Starch, Fujian Agriculture and Forestry University, Fuzhou, 350002, China

ARTICLE INFO

Keywords:
Lotus seed starch
Chitosan
Digestibility
Structural properties

ABSTRACT

The effect of chitosan (CS) on the *in vitro* digestibility and molecular structural properties of lotus seed starch (LS), and the correlation matrix was studied. The addition of CS could delay the hydrolysis of LS due to a increased level of slowly digestible starch (SDS). LS-CS blends exhibited lower pasting viscosity, greater amylose content and higher ordered structure than LS alone. A significant correlation was found between the digestibility and molecular structural properties of LS-CS blends. Rapidly digestible starch content was positively correlated with viscosity and full width at half-maximum height (FWHH) at 480 cm^{-1}; whereas, SDS content was negatively correlated with setback and FWHH. Moreover, CS concentration was positively related to absorbances at 1047 and 1035 $cm^{-1}$and amylose content. The results indicated that the addition of CS could be beneficial to the formation of an ordered molecular structure in LS-CS blends and decreased digestibility *in vitro*.

1. Introduction

Starch is the most important supply of carbohydrate-based energy in humans. It is consumed worldwide and contributes the largest proportion of the total caloric intake for populations in both western (50%) and developing countries (90%) (Xu et al., 2017). The rate at which starch is digested in the gastrointestinal tract, starch digestibility, is a major determinant of the human glycemic response and insulin levels after a meal. As suggested by Englyst et al. (1992), starch consists of different fractions: rapid digestible starch (RDS, digested in < 20 min), slowly digestible starch (SDS, digested in 20–120 min), and resistant starch (RS, digested in > 120 min). Nutritional guidance suggests that reducing the glycemic responses of carbohydrate-containing foods or consuming SDS- and RS-rich foods can benefit health by lowering the risk factors associated with developing chronic diseases (Augustin et al., 2015; Lehmann and Robin, 2007). Therefore, processing techniques have been developed to alter the enzymatic digestibility of starch to create food products with a low glycemic index.

Among these high amylose starch-modifying techniques, autoclaving-cooling treatments are effective in increasing RS content (Agama-Acevedo et al., 2018). The starch obtained from lotus (*Nelumbo nucifera*) seed, an important economic plant in Asia, is a high amylose starch containing approximately 40% (w/w) amylose (Guo et al., 2019; Zeng et al., 2009). An increased RS content found in autoclaving-cooling treated lotus seed starch (LS) is attributed to increased interactions between amylose molecules (Zhang et al., 2013). The autoclaving process destroys the crystal structure of the amylose molecules; whereas, the cooling process promotes rapid migration and reassociation of amylose molecules as double helices stabilized by hydrogen bonds (Zhang et al., 2014). This produces LS containing high RS fractions, which is highly resistant to amylase attack due to the presence of a more ordered structure (Zhang et al., 2013, 2014).

Other ingredients in the food matrix may also affect glucose metabolism by regulation of glucose absorption, the rate of gastric emptying, and gut hormone profiles (Berti et al., 2004). For instance, chitosan (CS), a natural polycationic polymer linked by D-glucosamine residues with functional groups (amino/acetamido groups), has been used extensively in food products to reduce fat absorption in the gastrointestinal tract (Helgason et al., 2008; Krajewska, 2004). According to Si et al. (2017), a high amylose maize starch and chitosan complex had a synergistic effect on obesity and diabetes prevention in rats fed with a high fat diet. The complex could control body weight and improve blood lipid composition more efficiently than starch or chitosan alone. Yang et al. (2017) reported that a combination of chitosan and whey

* Corresponding author. College of Food Science, Fujian Agriculture and Forestry University, Fuzhou, Fujian, 350002, PR China.
** Corresponding author. College of Food Science, Fujian Agriculture and Forestry University, Fuzhou, Fujian, 350002, China.
E-mail addresses: zyifst@163.com (Y. Zhang), zhlfst@163.com (H. Zeng).

https://doi.org/10.1016/j.fct.2019.110731
Received 29 April 2019; Received in revised form 1 July 2019; Accepted 28 July 2019
Available online 29 July 2019
0278-6915/

protein effectively reduces starch hydrolysis due to the enhanced long three-dimensional structure of the biopolymers. Autoclave-sterilization has been observed to induce an increase in crystallinity and higher equilibrium of chitosan-starch hydrogel (20/80 wt/wt), which was related to the intermolecular interactions of the blends and a decrease in ionic crosslinking density (Pereza et al., 2018). This would make the hydrogel appropriate to loading plant growth-promoting bacteria (PGPB), demonstrating great biotechnological potential as a delivery system for PGPB (Pereza et al., 2018). However, few studies have focused on the correlation between digestibility *in vitro* and structural properties of starch-chitosan blends by autoclaving-cooling treatment, or, in particular, visualization of the correlation matrix.

The objective of this paper was to investigate the effect of CS on the digestibility and molecular structural properties properties of LS and the correlation matrix. The effect of CS (0%, 0.20% and 0.40% w/w) on the *in vitro* digestibility of 6% w/w LS aqueous dispersions undergoing an autoclaving-cooling treatment were studied. The molecular structural properties were characterized using a Rapid Visco Analyzer, Raman microscopy, Fourier transform infrared spectroscopy (FTIR), and determining amylose contents. Furthermore, Pearson's correlations were applied to clarify the relationship between the *in vitro* digestibility and molecular structural properties of LS-CS blends and R software was utilized to visualize the correlation matrix.

2. Materials and methods

2.1. Materials

Lotus seeds were provided by Green Acres (Fujian) Food Co. Ltd. (Fujian, China) to prepare the starch (LS; total starch content 90.12%, moisture content 8.47%, protein content 0.98%, lipid content 0%) using previously published methods (Zhang et al., 2014; Zheng et al., 2019a). Carboxylated chitosan, CS (CAS-9012-76-4, Carboxylation 60–100%, viscosity 10–80 mPa s) was provided by Shanghai Macklin Biochemical Co., Ltd. (Shanghai, China). Amyloglucosidase (100,000 U/mL) was acquired from Aladdin Reagent Co. Ltd. (Shanghai, China), and α-amylase (10,000 U/mL) was provided by ANKOM (New York, USA). The amylose/amylopectin assay kit was purchased from Megazyme Co., Ltd. (Wicklow, Ireland). Dimethyl sulfoxide (DMSO, HPLC grade) was acquired from Sigma-Aldrich Chemical Co., Ltd. (MO, USA).

2.2. Preparation of LS and LS-CS blends by autoclaving-cooling treatment

Preparation of LS and LS-CS blends by autoclaving-cooling treatment was based on our previous study with some modifications (Zheng et al., 2019b. Aqueous solutions of CS [0%, 0.20%, and 0.40% (w/w)] were blended with 6% LS (w/w) and stirred mechanically for 30 min at room temperature. The mixtures were autoclaved at 121 °C for 30 min, then processed with the cooling storage at 4 °C for 7 days. Subsequently, the mixtures were freeze-dried at −81 °C for 48 h, ground, and passed through a 180-μm mesh screen (Shangyu Yinhe Testing Instrument Factory, Shaoxing, China).

2.3. In vitro digestion

The *in vitro* digestibility of LS and LS-CS blends by autoclaving-cooling treatment was analyzed using the method of Zheng et al., 2019a Each starch sample (200 mg) was dispersed in 10 mL acetate buffer solution (0.1 mol/L, pH 5.2), hydrolyzed by adding 10 mL mixed enzyme solution (α-amylase 200 U/mL, amyloglucosidase 160 U/mL) and stirred at 150 rpm in a water bath at 37 °C (DSHZ–300A, Taicang Testing Equipment Factory, Taicang, China). At each time point (0, 20, 40, 60, 90, 120, and 180 min), 0.5 mL of the hydrolysate was inactivated using 1.5 mL of 95% ethanol solution before being centrifuged at 6570 × *g* for 10 min. The aliquots of supernatant were adopted to determine the hydrolyzed glucose content using the 3,5-dinitrosalicylic acid method. According to the equations set out by Englyst et al. (1992), the hydrolysis rate, RDS, SDS, and RS contents were calculated using the following:

$$\text{Hydrolysis rate}\ (\%) = \frac{G_t \times 0.9}{TS} \times 100\% \quad (1)$$

$$\text{RDS}(\%) = \frac{(G_{20min} - G_{0min}) \times 0.9}{TS} \times 100\% \quad (2)$$

$$\text{SDS}(\%) = \frac{(G_{120\text{min}} - G_{20min}) \times 0.9}{\text{TS}} \times 100\% \quad (3)$$

$$\text{RS}(\%) = (1 - \text{RDS} - \text{SDS}) \times 100\% \quad (4)$$

where G_t is the amount of hydrolyzed glucose at time t. G_{0min}, G_{20min} and G_{120min} refer to the amount of glucose released within 0, 20, and 120 min, respectively. *TS* is the weight of the starch sample.

2.4. Pasting properties

The pasting properties of freeze-dried LS and LS-CS blends by autoclaving-cooling treatment were analyzed by a Rapid Visco Analyzer (S/N 2163595-TMB, Perten Instruments, NSW, Australia) using the previous method reported by Nawab et al. (2016). The temperature of the sample was equilibrated at 50 °C for 1 min, heated to 95 °C at a rate of 12 °C/min, held at 95 °C for 2.5 min, cooled to 50 °C at a rate of 12 °C/min, and held at 50 °C for 2 min. Meanwhile, the samples were automatic stirred at 960 rpm for 10 s and then at 160 rpm for the remainder of the experiment. The peak viscosity and setback viscosity were measured for the LS and LS-CS blends using TCW software. The peak viscosity was obtained at the point of maximum starch granular swelling, and setback viscosity was calculated as the difference between final viscosity and peak viscosity.

2.5. Amylose content

The amylose contents of the LS and LS-CS blends were determined using the amylose/amylopectin assay kits. 20 mg L sample was mixed with 1 mL DMSO, stirred, and heated for 15 min using boiling water bath. Then 95% (v/v) ethanol was used to precipitate the starch and the mixture was centrifuged at 2000 × *g* for 5 min. Then, 2 mL DMSO was added to redissolve the pellet, and heated in boiling water for 15 min. Concanavalin A solvent was used to precipitate the amylopectin and the supernatant was analyzed to determine the amylose content using the D-glucose (glucose oxidase/peroxidase) assay kits.

2.6. Raman microscopy

An Invia Raman confocal microscope (Invia Reflex, Renishaw, Gloucestershire, UK) was adopted to analyze the Raman spectra of the LS and LS-CS blends during digestion at 0, 20, and 120 min, using the method of Zhao et al. (2018). A 785-nm diode laser (500 mW) was employed. Spatial resolution was obtained using a 65-μm slit opening. The spectra range was 3200–100 cm^{-1} and the full width at half-maximum height (FWHH) at 480 cm^{-1} was used to characterize the ordered structure of starch using WiRE 4.2.

2.7. Short-range ordered structure based on FTIR

The short-range ordered structure of LS and LS-CS blends during digestion at 0, 20, and 120 min was characterized by the ratio of absorbance at 1047/1035 cm^{-1} ($R_{1047/1035}$) using FTIR (Nicolet 360, Thermo Nicolet Corporation, Madison, WI, USA). According to Zeng et al. (2017), 20 mg samples were mixed with 2000 mg potassium bromide (1:100, w/w) in an agate mortar, ground under an infrared lamp, then the mixture were pressed into a sheet using vacuum compression. The spectra range were recorded in 2000–800 cm^{-1} at a

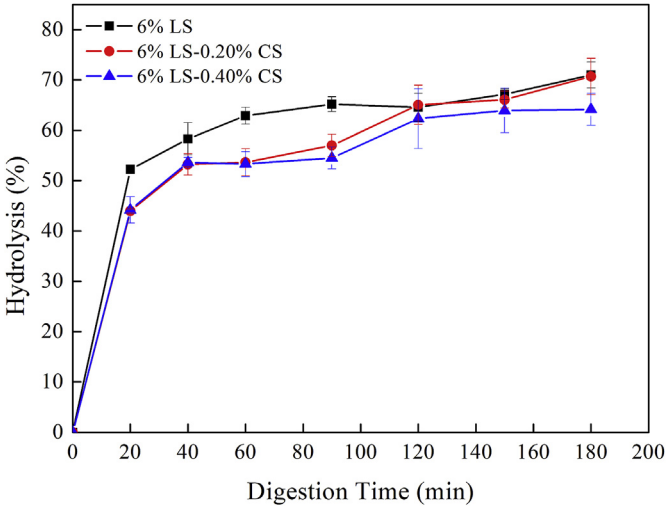

Fig. 1. The *in vitro* hydrolysis curves of LS and LS-CS blends by autoclaving-cooling treatment.

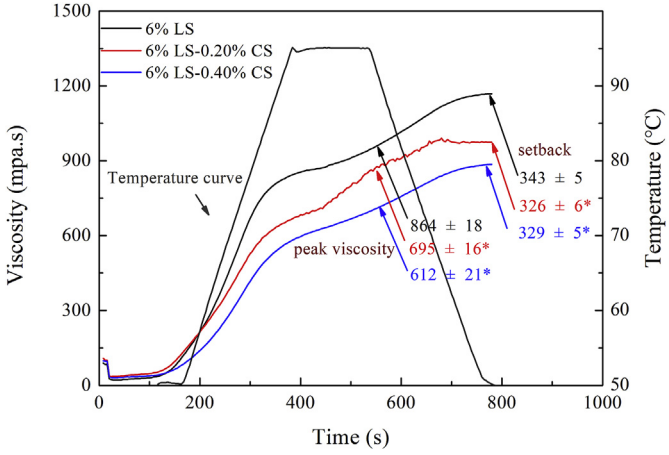

Fig. 2. Pasting curves of LS and LS-CS blends by autoclaving-cooling treatment.

resolution of 4 cm^{-1}.

2.8. Statistical analysis

All measurements were performed in triplicate and the data described above were expressed as mean values ± standard deviations. Data were analyzed using the DPS 9.50 system (Science Press, Beijing, China) with a least significant difference (LSD) test. A correlation matrix was visualized with the Pearson correlation coefficient using R software version 3.5.1. and RStudio (R Package, USA).

3. Results and discussion

3.1. In vitro digestion of LS-CS blends

The digestion rates of LS and LS-CS blends are shown in Fig. 1. Compared to LS alone, the starch granules of LS-CS blends exhibited slower digestion from 0 to 120 min followed by stable digestion after 120 min. And 6% LS-0.40% CS displayed a slightly lower rate of hydrolysis than LS and 6% LS-0.20% CS after 60 min of digestion. These results might be due to the content of each starch fraction (RDS, SDS, and RS). As shown in Table 1, the RDS content of LS significantly decreased with the addition of CS and the SDS content increased ($p < 0.05$); whereas, no distinct changes were found in the RS content compared with LS alone. In addition, in the concentration range of 0.20%–0.40%, CS had no significant effect on the starch fractions of LS. The results suggested that the addition of CS could slow the digestion rate of LS and increase SDS, which were expected to have several physiological benefits through a lower postprandial glycemic response (Diao et al., 2017; Yang et al., 2017).

3.2. Pasting properties of LS-CS blends

The pasting process is related to the absorption of water by starch and involves granular swelling and disruption. The stability of the paste is tested by heating and cooling (Fonseca-Florido et al., 2018; Nawab et al., 2016). The pasting properties of freeze-dried LS and LS-CS blends by autoclaving-cooling treatment are presented in Fig. 2. The results showed that the viscosity of LS decreased following the addition of CS during pasting processing. With the addition of 0.20% and 0.40% CS, the peak viscosities of the LS blends decreased from 864 ± 18 to 695 ± 16 and 612 ± 21 mPa s, respectively ($p < 0.05$). Furthermore, the setback of the LS blends decreased from 343 ± 5 to 326 ± 6 and 329 ± 5 mPa s with the additions of 0.20% and 0.40% CS, respectively ($p < 0.05$). Generally, the decrease in viscosity of starches with heating-cooling treatment (like annealing and autoclaving-cooling treatment) may be attributed to the strengthened molecular organization or interactions between starch chains, which reduce the extent of hydration in the amorphous regions and restrict swelling ability (Kim and Kwak, 2010; Xu et al., 2018). Thus, the decreased viscosity of LS-CS blends might be due to the enhanced structural order in the starch granules. Decreases in paste viscosity have also been found in chitosan-modified waxy maize starches. This may be attributable to the formation of ester bonds by the interactions of chitosan with maize starch and the progressive organization of the starch structure following these interactions leading to limitations in starch swelling and granule disruption of the autoclaving-cooling treated LS-CS blends (Diao et al., 2017).

3.3. Amylose contents of LS-CS blends

Starch is made up of glucose units extended with (1 → 4)-α linear glycosidic linkages and branched with (1 → 6)-α glycosidic linkages, including the amylose (largely linear with a few long-chain branches) and amylopectin (hyperbranched with numerous short chains) molecules. In the defatted or low lipid starch, some amylose molecules form double helices, which are highly resistant to enzymatic digestion, while the remaining amylose remains in the amorphous region of starch (Biliaderis, 2009; Man et al., 2012). The amylose contents of LS and LS-CS blends with autoclaving-cooling treatment are presented in Table 1. The amylose of LS by autoclaving-cooling treatment was 32.03 ± 3.17%. The amylose contents of LS-CS blends were much

Table 1
Starch fractions and amylose contents of LS and LS-CS blends by autoclaving-cooling treatment *in vitro* digestion (% total starch).

	RDS	SDS	RS	Amylose contents
6% LS	52.24 ± 0.86^{a}	12.34 ± 3.43^{b}	35.43 ± 2.76^{a}	32.03 ± 3.17^{b}
6% LS-0.20% CS	43.97 ± 0.42^{b}	21.08 ± 4.27^{a}	34.95 ± 3.88^{a}	43.19 ± 2.43^{a}
6% LS-0.40% CS	44.19 ± 2.64^{b}	18.13 ± 1.64^{a}	37.68 ± 5.90^{a}	44.38 ± 3.06^{a}

Values with different superscript lowercase letters in the same column are significantly different ($p < 0.05$).

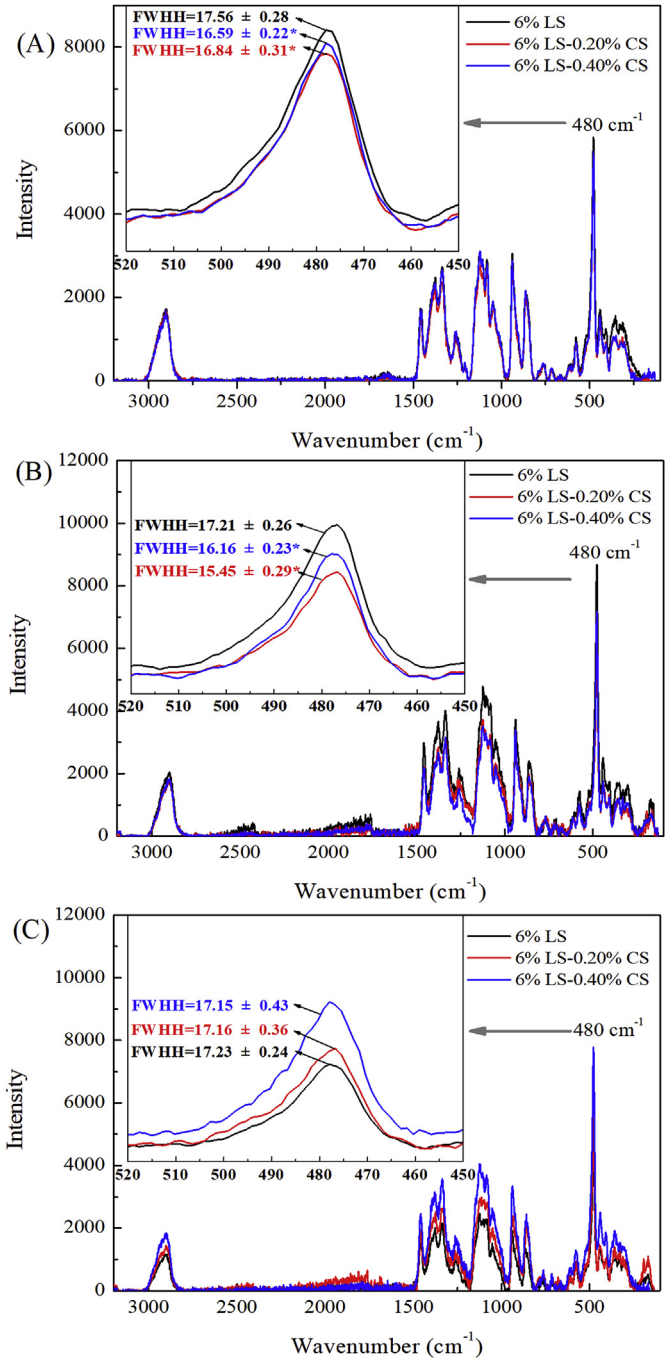

Fig. 3. Raman spectra of LS and LS-CS blends by autoclaving-cooling treatment: (A) starches without digestion; (B) starch residues digested for 20 min; (C) starch residues digested for 120 min.

higher than those of LS alone; the contents were up to 43.19 ± 2.43% and 44.38 ± 3.06% in 6% LS-0.20% CS and 6% LS-0.40% CS, respectively ($p < 0.05$). These results may be due to the presence of gum, which promotes adhesive interactions among the gelatinized starch granules (Mandala and Bayas, 2004). This enhances the forces applied to the blends and facilitates water entry (swelling), which leads to the solubilization and exudation of amylose when subjected to an autoclaving processing, cuasing the amylose contents of LS-CS blends greater than LS alone. And this phenomenon has been observed in our previous study using an atomic force microscope and confocal laser scanning microscopy, the increased amylose contents led to the greater molecular alignment and aggregation of starch molecules, accelerating reorganization of starch structural gels (Zheng et al., 2019c.

3.4. Raman spectra of LS-CS blends

The Raman spectra of LS and LS-CS blends by autoclaving-cooling treatment are presented in Fig. 3. For all samples, several clear characteristic bands could be seen at 2910, 1335, 1264, 1143, 1084, 1053, 943, 856, and 480 cm^{-1}. No new Raman peaks were found in LS-CS blends. The band at 480 cm^{-1} was related to the stretching vibration of the C–O–C ring bond (Zhao et al., 2018). The FWHH of this band could measure the structural variation and crystallinity of starch samples, and the lower the FWHH, the higher the molecular order of the starch (Zhao et al., 2018). Compared to LS (17.56 ± 0.28 cm^{-1}) at 0 min, the FWHH values (see Fig. 3) for 6% LS-0.20% CS and 6% LS-0.40% CS blends decreased to 16.84 ± 0.22 and 16.59 ± 0.31 cm^{-1}, respectively. This indicated that the molecular order or crystallinity of LS increased with the addition of CS. This might be owing to the increase in amylose content, which could promote amylose crystallization and form an ordered matrix, thus accelerating the aggregation and crystallization of amylopectin during long-term retrogradation (Fechner et al., 2005). Raguzzoni et al. (2016) have reported that the long-term retrogradation of starch is slightly increased by CS addition, which might be a result of phase rearrangements between starch and chitosan in short-time scales.

Moreover, the FWHH values of the Raman band at 480 cm^{-1} were reported to be negatively correlated with the digestibility of starch (Zhao et al., 2018). In this paper, after 20 min of *in vitro* digestion, the FWHH values of the Raman band at 480 cm^{-1} of 6% LS, 6% LS-0.20% CS and 6% LS-0.40% CS samples were 17.21 ± 0.26, 16.16 ± 0.23, and 15.45 ± 0.29 cm^{-1}, respectively. After 120 min of digestion, the FWHH values of the Raman band at 480 cm^{-1} of 6% LS, 6% LS-0.20% CS and 6% LS-0.40% CS increased to 17.23 ± 0.24, 17.16 ± 0.36, and 17.15 ± 0.43 cm^{-1}, respectively. These results indicated that the ordered structure of starch increased during the initial enzymatic digestion and then decreased rapidly. Similar phenomena have been reported in banana starch (Jiang et al., 2015) and high amylose rice starch (Man et al., 2012), where the crystalline degree of the starches increased during the initial digestion and then decreased rapidly during the following digestion. This could be attributed to the initial hydrolysis of the amorphous region, which led to a relatively high content of the crystalline region or the reordering of the chain segments deriving from cleavage of the amorphous starch chains (Man et al., 2012). There was no significant difference in the FWHH values of the Raman band at 480 cm^{-1} between LS and LS-CS blends after digestion for 120 min, which concurred with the similar RS content in the different LS samples.

3.5. Short-range ordered molecular structure by FTIR

To further identify the changes in the short-range ordered molecular structure of the LS and LS-CS blends with autoclaving-cooling treatment, the spectra and $R_{1047/1035}$ of LS and LS-CS blends after *in vitro* digestion were obtained based on FTIR (see Fig. 4). LS samples showed similar typical bands of starch at 1645, 1154, 1081, 1021, 929, and 854 cm^{-1}. Compared to LS alone (Fig. 4A), LS-CS blends showed a new peak located at 1569.77 cm^{-1}, which is attributed to amide-NH_2 absorption. These results concurred with a previous report, which suggested that interactions might occur between the hydroxyl groups of starch and the amino groups of chitosan (Diao et al., 2017). The new peak, however, nearly disappeared after enzymatic digestion (Fig. 4 B and C). It appeared to be hydrolyzed easily with no apparent relationship between the FTIR spectrum pattern and digestibility. $R_{1047/1035}$ values of LS-CS blends rose with increasing concentrations of CS ($p < 0.05$). This indicated that CS addition could increase short-range orders of LS with autoclaving-cooling treatment and this was consistent with the Raman behavior. During digestion, the changes in $R_{1047/1035}$

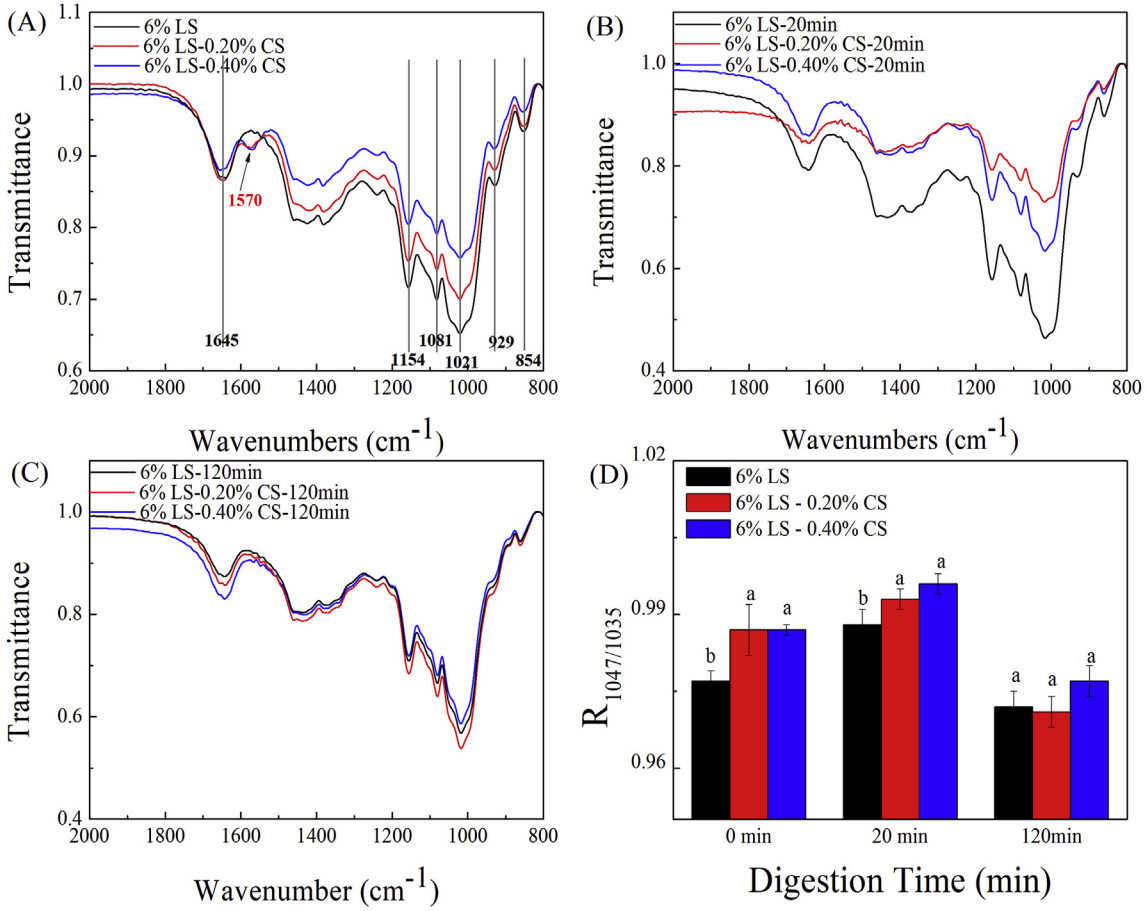

Fig. 4. FTIR spectra of LS and LS-CS blends by autoclaving-cooling treatment: (A) starches without digestion; (B) starch residues digested for 20 min; (C) starch residues digested for 120 min; (D) Short-range ordered structures (the ratio between 1047 cm^{-1} and 1035 cm^{-1} absorbances: $R_{1047/1035}$).

were also similar to the FWHH values of the Raman band at 480 cm^{-1} for all LS samples, which increased after 20 min of digestion and then decreased after 120 min of digestion. We found that the changes in ordered structure with digestion concurred with the LS hydrolysis and starch fractions of the granules. Compared with LS alone, the higher $R_{1047/1035}$ and lower FWHH values for the initial LS-CS blends and starch residues after 20 min of digestion suggested that a more ordered structure was present in these starches and this was closely related to their decreased RDS and increased SDS contents. After 120 min of digestion, it appeared that there was no further significant difference in the ordered structure due to the similar RS contents of LS and LS-CS blends.

3.6. Pearson's correlation between digestibility and molecular structural properties of LS-CS blends

Based on Pearson's correlations and R software, the correlation matrix between digestibility *in vitro* and the molecular structural properties of LS-CS blends by autoclaving-cooling treatment are shown in Fig. 5. The RDS content showed significant positive correlations with peak viscosity ($p < 0.01$), setback ($p < 0.01$), and FWHH ($p < 0.05$) and significant negative correlations with $R_{1047/1035}$ ($p < 0.01$) and amylose ($p < 0.01$). At the same time, the SDS content demonstrated significant negative correlation with setback ($p < 0.01$), and FWHH of the Raman band at 480 cm^{-1} ($p < 0.01$). This revealed that the stable structure formed by the higher molecular order resisted enzyme attack, resulting in a significant decrease in RDS and an increase in SDS. Furthermore, the CS concentration was negatively correlated with peak viscosity ($p < 0.01$), setback ($p < 0.05$), and the FWHH of the Raman band at 480 cm^{-1} ($p < 0.01$), however, it was positively correlated with amylose ($p < 0.01$) and $R_{1047/1035}$ ($p < 0.01$). This indicated that the addition of CS could cause a decline in viscosity and increases in the amylose content and ordered structures of LS. During autoclaving, starch granules are fully hydrated and swollen at high temperatures (121 °C) in the presence of excess moisture. The ordered chain domains of amylopectin and crystallites are destabilized and melt cooperatively, causing amylose leaching (Biliaderis, 2009). With the addition of CS, the increased amylose may promote structural reordering and reorganization in LS, which was suggested by the positive correlation between the amylose content and $R_{1047/1035}$ values ($p < 0.05$) and the negative correlation with the FWHH of the Raman band at 480 cm^{-1} ($p < 0.05$). One consequence of conformational ordering and aggregation of double helical chain segments in retrograded amylose is their resistance to enzyme-catalyzed hydrolysis (Biliaderis, 2009). As confirmed by previous studies, high molecular order and relative crystallinity could lead to a low rate of enzymatic hydrolysis (Ding et al., 2018; Hao et al., 2018). A negative correlation was found between the viscosity (e.g. peak viscosity and setback) and ordered structures of LS-CS blends, as the viscosity was negatively correlated with $R_{1047/1035}$ ($p < 0.01$) and positively correlated with the FWHH of the Raman band at 480 cm^{-1} ($p < 0.01$). Again, this may be attributable to the formation of ester bonds between chitosan and starch causing the more organized structure and lower viscosity of the blends (Diao et al., 2017). Furthermore, as reported by Han and Bemiller (2007), the increased peak viscosity suggested that the starch granule structure might be loosened to become more readily hydrated and swollen, which resulted in greater total digestibility. Conversely, the decreased viscosity indicated that LS-CS blends would be more stable

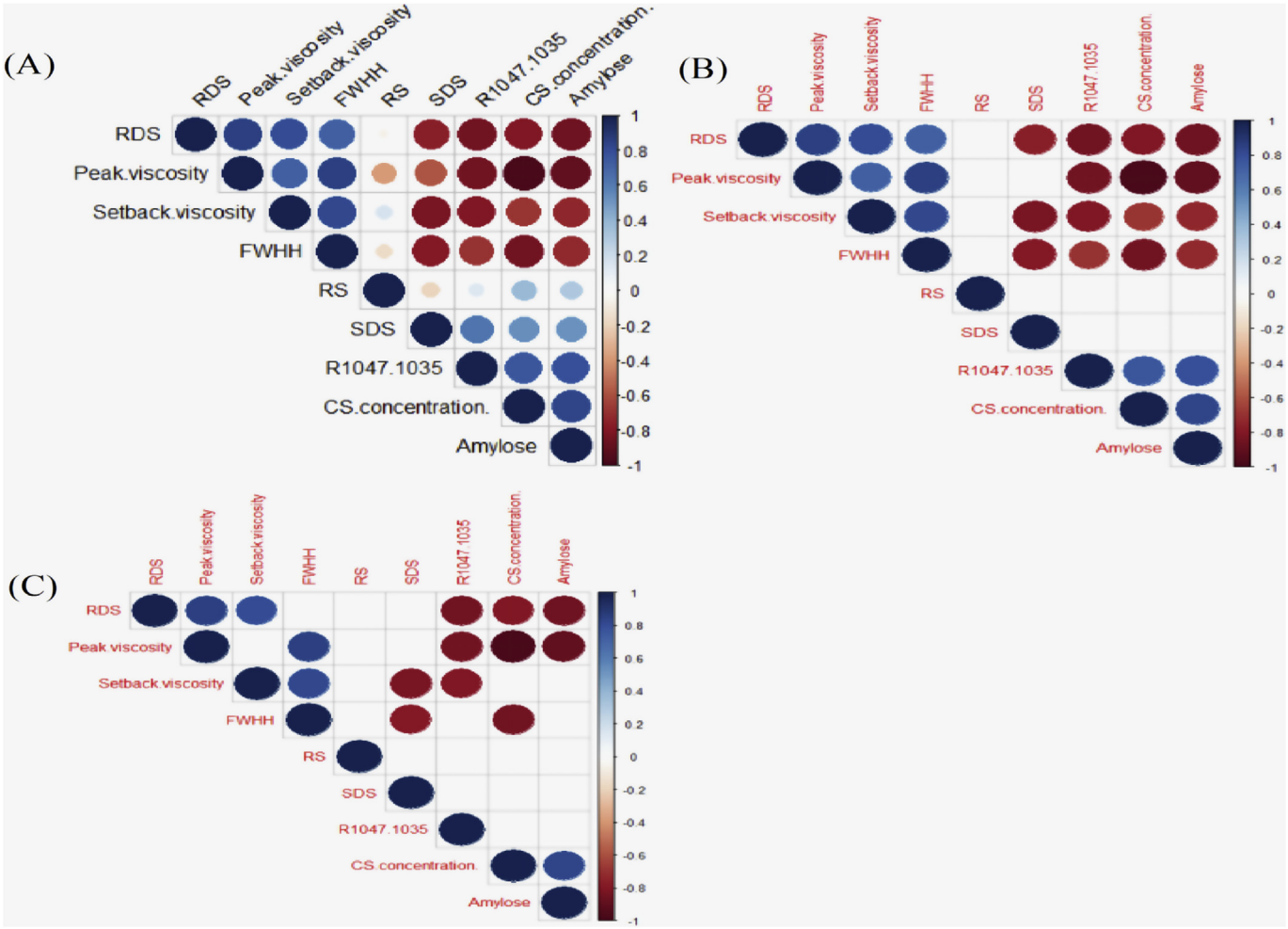

Fig. 5. The correlation matrix between digestibility *in vitro* and molecular structural properties of LS-CS blends by autoclaving-cooling treatment: (A) the whole correlation matrix; (B) the correlation matrix at $p < 0.05$; (C) the correlation matrix at $p < 0.01$. The ruler represents Pearson's correlation coefficient r.

and less swollen, limiting the accessibility of starch to enzyme attack, thus causing a decrease in RDS and an increase in SDS during digestion. Therefore, the viscosity was observed to be significantly correlated with the RDS and SDS contents of LS-CS blends. However, the RS content of LS was not affected by the addition of CS and the changes of structural properties (i.e. viscosity, amylose content, and ordered structure; $r < 0.05$, $p > 0.05$). This reasons for these needs to be further investigated.

Henceforth, it can be assumed that the higher amylose in LS-CS blends by autoclaving treatment promoted rapid retrogradation (i.e. the structural reordering and reorganization of gelatinized starch) of amylose, which accelerated amylopectin retrogradation during long-term cooling storage. Furthermore, the more stable matrix with higher ordered structure observed in the pasting behavior and Raman and FTIR analyses, resulted in increased SDS and decreased RDS contents of LS-CS blends.

4. Conclusions

The *in vitro* digestibility and molecular structural properties of LS-CS blends by autoclaving-cooling treatment were studied. The results showed that the digestion rate of LS was decreased by adding CS, which contributed to a decrease in RDS and an increase in SDS. The changes in $R_{1047/1035}$ and FWHH values suggested that the more ordered structures of the initial LS-CS blends and their residues after 20 min of digestion were closely related to their decreased RDS and increased SDS contents. While following 120 min of digestion, no significant difference in the ordered structure led to similar RS contents in LS and LS-CS blends. The Pearson's correlation analysis further confirmed that the decreased RDS was negatively related to amylose content and $R_{1047/1035}$ (short-range ordered structure); whereas, the SDS content was significantly negatively related to the setback and FWHH value of the Raman band at 480 cm^{-1}. The results suggested that CS was capable of modifying the digestibility of amylose-rich starches by autoclaving-cooling treatment, which could be applied to produce significant amounts of SDS and RS for the development of healthy, functional foodstuffs.

Declaration of interests

The authors declare that they have no known competing financial interests or personal relationships that could have appeared to influence the work reported in this paper.

Acknowledgement

This study was financially supported by the Scientific Research Foundation of the Graduate School of Fujian Agriculture and Forestry University (Grant number YB2018009), the Project of International Cooperation and Exchanges in Science and Technology of Fujian Agriculture and Forestry University (Grant number KXGH17001), Leading Talents Support Program of Science and Technology Innovation in Fujian Province (Grant number KRC16002A), the Support Project for Distinguished Young Scholars of Fujian Agriculture and Forestry University (Grant number xjq201714), the Science and

Technology Innovation Project of Fujian Agriculture and Forestry University (Grant number CXZX2017414).

References

Agama-Acevedo, E., Pacheco-Vargas, G., Bello-Perez, L.A., Alvarez-Ramirez, J., 2018. Effect of drying method and hydrothermal treatment of pregelatinized Hylon VII starch on resistant starch content. Food Hydrocolloids 77, 817–824. https://doi.org/10.1016/j.foodhyd.2017.11.025.

Augustin, L.S., Kendall, C.W., Jenkins, D.J., Willett, W.C., Astrup, A., Barclay, A.W., Björck, I., Brand-Miller, J.C., Brighenti, F., Buyken, A.E., 2015. Glycemic index, glycemic load and glycemic response: an international scientific consensus summit from the international carbohydrate quality consortium (ICQC). Nutr. Metab. Cardiov. 25 (9), 795–815. https://doi.org/10.1016/j.numecd.2015.05.005.

Berti, C., Riso, P., Monti, L.D., Porrini, M., 2004. In vitro starch digestibility and in vivo glucose response of gluten-free foods and their gluten counterparts. Eur. J. Clin. Nutr. 43 (4), 198–204. https://doi.org/10.1007/s00394-004-0459-1.

Biliaderis, C.G., 2009. Chapter 8 – structural transitions and related physical properties of starch. Starch 293–372. https://doi.org/10.1016/B978-0-12-746275-2.00008-2.

Diao, Y., Xu, S., Shang, W., Zhou, Z., Wang, Z., Zheng, P., Strappe, P., Blanchard, C., 2017. Effect of interactions between starch and chitosan on waxy maize starch physicochemical and digestion properties. CyTA - J. Food 15 (3), 327–335. https://doi.org/10.1080/19476337.2016.1255916.

Ding, Y., Lin, Q., Kan, J., 2018. Development and characteristics nanoscale retrograded starch as an encapsulating agent for colon-specific drug delivery. Colloids Surf., B 171, 656–667. https://doi.org/10.1016/j.colsurfb.2018.08.007.

Englyst, H.N.N., Kingman, S.M.M., Cummings, J.H.H., 1992. Classification and measurement of nutritionally important starch fractions. Eur. J. Clin. Nutr. 46, S33–S50. https://doi.org/10.1128/IAI.01649-06.

Fechner, P.M., Wartewig, S., Kleinebudde, P., Neubert, R.H., 2005. Studies of the retrogradation process for various starch gels using Raman spectroscopy. Carbohydr. Res. 340 (16), 2563–2568. https://doi.org/10.1016/j.carres.2005.08.018.

Fonseca-Florido, H.A., Gomez-Aldapa, C.A., Lopez-Echevarría, G., Velazquez, G., Morales-Sanchez, E., Castro-Rosas, J., Mendez-Montealvo, G., 2018. Effect of granular disorganization and the water content on the rheological properties of amaranth and achira starch blends. LWT - Food Sci. Technol. (Lebensmittel-Wissenschaft -Technol.) 87, 2080–2286. https://doi.org/10.1016/j.lwt.2017.09.004.

Guo, Z., Jia, X., Lin, X., Chen, B., Sun, S., Zheng, B., 2019. Insight into the formation, structure and digestibility of lotus seed amylose-fatty acid complexes prepared by high hydrostatic pressure. Food Chem. Toxicol. 128, 81–88. https://doi.org/10.1016/j.fct.2019.03.052.

Han, J.A., Bemiller, J.N., 2007. Preparation and physical characteristics of slowly digesting modified food starches. Carbohydr. Polym. 67 (3), 366–374. https://doi.org/10.1016/j.carbpol.2006.06.011.

Hao, H., Li, Q., Bao, W., Wu, Y., Ouyang, J., 2018. Relationship between physicochemical characteristics and in vitro digestibility of chestnut (*Castanea mollissima*) starch. Food Hydrocolloids 84, 193–199. https://doi.org/10.1016/j.foodhyd.2018.05.031.

Helgason, T., Weiss, J., Mcclements, D.J., Gislason, J., Einarsson, J.M., Thormodsson, F.R., Kristbergsson, K., 2008. Examination of the interaction of chitosan and oil-in-water emulsions under conditions simulating the digestive system using confocal microscopy. J. Aquat. Food Prod. Technol. 17 (3), 216–233. https://doi.org/10.1080/10498850802179784.

Jiang, H., Zhang, Y., Hong, Y., Bi, Y., Gu, Z., Cheng, L., Li, Z., Li, C., 2015. Digestibility and changes to structural characteristics of green banana starch during invitro digestion. Food Hydrocolloids 49 (3), 192–199. https://doi.org/10.1016/j.foodhyd.2015.03.023.

Kim, S., Kwak, J., 2010. Formation of resistant starch in corn starch and estimation of its content from physicochemical properties. Starch - Stärke 61, 514–519. https://doi.org/10.1002/star.200800120.

Krajewska, B., 2004. Application of chitin- and chitosan-based materials for enzyme immobilizations: a review. Enzym. Microb. Technol. 35 (2), 126–139. https://doi.org/10.1016/j.enzmictec.2003.12.013.

Lehmann, U., Robin, F., 2007. Slowly digestible starch - its structure and health implications: a review. Trends Food Sci. Technol. 18 (7), 346–355. https://doi.org/10.1016/j.tifs.2007.02.009.

Man, J., Yang, Y., Zhang, C., Zhou, X., Dong, Y., Zhang, F., Liu, Q., Wei, C., 2012. Structural changes of high-amylose rice starch residues following in *vitro* and in *vivo* digestion. J. Agric. Food Chem. 60 (36), 9332–9341. https://doi.org/10.1021/jf302966f.

Mandala, I.G., Bayas, E., 2004. Xanthan effect on swelling, solubility and viscosity of wheat starch dispersions. Food Hydrocolloids 18 (2), 191–201. https://doi.org/10.1016/S0268-005X(03)00064-X.

Nawab, A., Alam, F., Haq, M.A., Hasnain, A., 2016. Effect of guar and xanthan gums on functional properties of mango (Mangifera indica) kernel starch. Int. J. Biol. Macromol. 93, 630–635. https://doi.org/10.1016/j.ijbiomac.2016.09.011.

Pereza, J.J., Francois, N.J., Maroniche, G.A., Borrajo, M.P., Pereyr, M.A., Creus, C.M., 2018. A novel, green, low-cost chitosan-starch hydrogel as potential delivery system for plant growth-promoting bacteria. Carbohydr. Polym. 202, 409–417. https://doi.org/10.1016/j.carbpol.2018.07.084.

Raguzzoni, J.C., Delgadillo, I., Silva, J.A.L.D., 2016. Influence of a cationic polysaccharide on starch functionality. Carbohydr. Polym. 150, 369–377. https://doi.org/10.1016/j.carbpol.2016.05.024.

Si, X., Strappe, P., Blanchard, C., Zhou, Z., 2017. Enhanced anti-obesity effects of complex of resistant starch and chitosan in high fat diet fed rats. Carbohydr. Polym. 157, 834–841. https://doi.org/10.1016/j.carbpol.2016.10.042.

Xu, J., Kuang, Q., Wang, K., Zhou, S., Wang, S., Liu, X., Wang, S., 2017. Insights into molecular structure and digestion rate of oat starch. Food Chem. 220, 25–30. https://doi.org/10.1016/j.foodchem.2016.09.191.

Xu, M., Saleh, A.S.M., Yu, L., Jing, L., Zhao, K., Hao, W., Zhang, G., Yang, S.O., Li, W., 2018. The changes in structural, physicochemical, and digestive properties of red adzuki bean starch after repeated and continuous annealing treatments. Starch - Stärke 1700322. https://doi.org/10.1002/star.201700322.

Yang, N., Ashton, J., Gorczyca, E., Kasapis, S., 2017. In-vitro starch hydrolysis of chitosan incorporating whey protein and wheat starch composite gels. Heliyon 3 (10) e00421. https://doi.org/10.1016/j.heliyon.2017.e00421.

Zeng, H., Huang, C., Chen, P., Zheng, B., Liu, J., Zhang, Y., 2017. Comparative study on the structural and physicochemical properties of flour and starch from *Dioscorea opposita* Thunb. Chin. J. Struct. Chem. 36 (11), 1825–1836. https://doi.org/10.14102/j.cnki.0254-5861.2011-1768.

Zeng, S., Zheng, B., Lin, Y., Zhou, X.H., 2009. Granular characteristics of lotus-seed starch. J. Chin. Cereals Oils. Assoc. 8, 62–64. http://en.cnki.com.cn/Article_en/CJFDTOTAL-ZLYX200908013.htm.

Zhang, Y., Wang, Y., Zheng, B., Lu, X., Zhuang, W., 2013. The in vitro effects of retrograded starch (resistant starch type 3) from lotus seed starch on the proliferation of Bifidobacterium adolescentis. Food & Funct. 4 (11), 1609–1616. https://doi.org/10.1039/C3FO60206K.

Zhang, Y., Zeng, H.L., Wang, Y., Zeng, S., Zheng, B., 2014. Structural characteristics and crystalline properties of lotus seed resistant starch and its prebiotic effects. Food Chem. 155 (19), 311–318. https://doi.org/10.1016/j.foodchem.2014.01.036.

Zhao, J., Zhang, Y., Wu, Y., Liu, L., Ouyang, J., 2018. Physicochemical properties and in *vitro* digestibility of starch from naturally air-dried chestnut. Int. J. Biol. Macromol. 117, 1074–1080. https://doi.org/10.1016/j.ijbiomac.2018.06.034.

Zheng, M., Su, H., Luo, M., Shen, J., Zeng, S., Zheng, B., Zeng, H., Zhang, Y., 2019a. Effect of hydrocolloids on the retrogradation of lotus seed starch undergoing an autoclaving-cooling Treatment. J. Food Sci. 84, 466–474. https://doi.org/10.1111/1750-3841.14480.

Zheng, M., Su, H., You, Q., Zeng, S., Zheng, B., Zhang, Y., Zeng, H., 2019b. An insight into the retrogradation behaviors and molecular structures of lotus seed starch-hydrocolloid blends. Food Chem. 295, 548–555. https://doi.org/10.1016/j.foodchem.2019.05.166.

Zheng, M., You, Q., Lin, Y., Lan, F., Luo, M., Zeng, H., Zheng, B., Zhang, Y., 2019c. Effect of guar gum on the physicochemical properties and in vitro digestibility of lotus seed starch. Food Chem. 272, 286–291. https://doi.org/10.1016/j.foodchem.2018.08.029.